

Addition of deep brain stimulation signal to a local field potential driven Izhikevich model masks the pathological firing pattern of an STN neuron

Kostis P. Michmizos, *Student Member IEEE*, Konstantina S. Nikita, *Senior Member, IEEE*

Abstract—The crucial engagement of the subthalamic nucleus (STN) with the neurosurgical procedure of deep brain stimulation (DBS) that alleviates medically intractable Parkinsonian tremor augments the need to refine our current understanding of STN. To enhance the efficacy of DBS as a result of precise targeting, STN boundaries are accurately mapped using extracellular microelectrode recordings (MERs). We utilized the intranuclear MER to acquire the local field potential (LFP) and drive an Izhikevich model of an STN neuron. Using the model as the test bed for clinically acquired data, we demonstrated that stimulation of the STN neuron produces excitatory responses that tonically increase its average firing rate and alter the pattern of its neuronal activity. We also found that the spiking rhythm increases linearly with the increase of amplitude, frequency, and duration of the DBS pulse, inside the clinical range. Our results are in agreement with the current hypothesis that DBS increases the firing rate of STN and masks its pathological bursting firing pattern.

I. INTRODUCTION

HIGH - frequency deep brain stimulation (DBS) of the basal ganglia is an effective therapeutic avenue for patients with medically intractable movement disorders. It involves implanting an electrode into the target area within the brain and connecting it to an internal pulse generator usually located in the chest area. The insertion of an electrode into one of the pivotal nuclei of the basal ganglia, the subthalamic nucleus (STN), is becoming a notable treatment of the cardinal motor features of Parkinson's disease (PD) (resting tremor, rigidity, bradykinesia) [1] since the clinical benefits of the procedure are analogous to those achieved by surgical lesioning ([2], [3]). Although DBS has been effective in the treatment of many movement disorders and is rapidly being explored for the treatment of other neurologic disorders, the understanding of its mechanisms in the cellular level remains unclear and continues to be debated in the scientific community. However, it is the identification of these mechanisms on which the optimization and the efficacy of DBS treatment will depend on.

Currently, the efficacy of the method is macroscopically guarded by the precise targeting of a microelectrode within the STN. The exact location is usually estimated by a

neurologist during surgery, observing the neuronal activity which is recorded from the nearby area, displayed on an oscilloscope and usually played on an audio monitor. Oddly enough, this procedure provides a unique opportunity for recording neural activity as close to its generator as possible allowing maximal spatial resolution and accuracy for the microelectrode recordings (MERs).

Contradictory hypotheses for the therapeutic effect of DBS to various medical conditions, including intractable tremor [4], dystonia [5], epilepsy [6] and obsessive-compulsive disorder [7], led to long-standing scientific disputes. Trying to answer how high-frequency DBS works leads to a paradox of how stimulation (traditionally believed to activate neurons) can result in similar therapeutic outcomes as lesioning target structures. In general, there exist two main philosophies for DBS explanation: (1) DBS generates a functional ablation by suppressing or inhibiting the structure being stimulated or (2) DBS results in activation of the stimulated structures that are transmitted throughout the network [8]. In line with these philosophies, there exist four general hypotheses that are used to explain the mechanisms of DBS: (1) depolarization blockade [9]; (2) synaptic inhibition [10]; (3) synaptic depression [11]; and (4) stimulation-induced modulation of pathologic network activity [12]. However, it seems that the therapeutic mechanisms underlying DBS most likely represent a combination of several phenomena [13].

The aim of the present study is to utilize the local field potentials (LFPs) acquired from single neuron MERs to create an Izhikevich model of an STN neural cell. We introduce for the first time the superposition of a DBS signal and the LFP to drive the Izhikevich model. The simulation results can be used to shed some light into the effects of the DBS on the cellular level.

II. MODELING THE STN NEURON ACTIVITY

A. Single neuron MER analysis

MER's acquisition, processing and analysis are analytically described elsewhere ([14]-[15]). Data used in this study were obtained from a PD patient, during DBS operation. Two single neuron MERs are included in this study. The signals, acquired around the final stimulation point (+/- 1mm) inside the STN, exhibited the typical STN discharge pattern (intense irregular neuronal activity with increased background activity and bursting spike trains

K.P. Michmizos and K.S. Nikita are with the Biomedical Simulations and Imaging Laboratory, Faculty of Electrical and Computer Engineering, National Technical University of Athens, 15780, Athens, Greece (corresponding author: Kostis Michmizos, tel: +30-210-7721597; fax: +30-210-7722320; e-mail: konmic@biosim.ntua.gr).

usually present [16]).

Off-line data processing and analysis were conducted by custom-made MATLAB (The MathWorks, Natick, MA) code. An FIR equiripple low-pass (LP) filter of order of 2100 samples, with a pass-band of [0 100] Hz and a stop-band of [0.15 12] kHz and p-p rippling in passband equal to 2×10^{-6} db was used to acquire the LFP signal. The short duration of an AP (about 1 ms) was ignored. Hence, an AP sequence was characterized simply by a binary signal in which the ones represent the times when spikes occurred.

B. The Izhikevich model neuron

The differential equations that describe the Izhikevich model are [17]:

$$\frac{dv}{dt} = 0.04v^2 + 5v + 140 - u + I \quad (1)$$

$$\frac{du}{dt} = a(bv - u) \quad (2)$$

with the auxiliary after-spike resetting

$$\text{If } v \geq +30 \text{ mV, then } v \leftarrow c \text{ and } u \leftarrow u + d. \quad (3)$$

In the above equations, $a, b, c,$ and d are abstract parameters of the model discussed in [17], v is the membrane voltage potential of the neuron, u represents a membrane recovery variable providing negative feedback to v . For the Izhikevich model to exhibit a discharge mode that matches an STN glutamatergic projection neuron, its parameter values should be set as follows: $a = 0.005$, $b = 0.265$, $c = -65$, $d = 1.5$ [18]. Alternatively, the parameters defined for tonic spiking ($a = 0.02$, $b = 0.2$, $c = -65$, $d = 6$) [17] may also be used with comparable accuracy.

In the model, synaptic currents or injected dc-currents are delivered via the variable I . If we assume that the source region volume is much smaller than the distance to the microelectrode and that the extracellular fluid is an infinite, homogeneous, isotropic, and purely resistive volume conductor, the LFP measured externally to a source region could be described as:

$$LFP(t) = \frac{1}{4\pi\sigma} \frac{I(t)}{|\mathbf{r}|} \quad (4)$$

where $I(t)$ is the current sources that contribute to the recorded LFP, \mathbf{r} is the distance of each current source to the microelectrode, and σ is the macroscopic electrical conductivity of the extracellular space. The current, I , injected into the Izhikevich model, can now be described by the linear transformation $I = \kappa \cdot LFP$ where $\kappa = 4\pi\sigma|\mathbf{r}|$. In other words, we assume that the sum of the currents in the dendritic sites that results to the recorded LFP is directly proportional to the LFP.

C. Model validation

We quantitatively compare the agreement between the spike train predicted from the model and the spike train detected from the MERs. The first approach is to plot the empirical cumulative distribution function (CDF) of the detected spiking times against the CDF of the predicted spiking times. If the model accurately predicts the recorded spikes, then the plot follows a 45° line. If the model fails to

account for some aspect of the spiking behavior, then that lack of fit is reflected in the plot as a significant deviation from the 45° line.

A second approach is to estimate the agreement between the model and data by constructing a sorted interspike interval (ISI) plot. The predicted sorted ISIs are plotted against those acquired by MERs. These plots are used for visualizing which ISIs of the recorded data are well captured and which are poorly captured by the model. Such comparisons are especially useful in testing the ability of the model to predict valuable characteristics of an STN neuron, such as the onset and the recession of a bursting spike train.

Finally, we are interested not only in the exact timing of each spike, but also in the rhythm of the neural activity. In order to validate the model in terms of rhythm prediction, we calculated the number of spikes present in adjacent, non-overlapping bins. The bin width, for this study, was kept equal to 5 ms.

D. Superposition of the DBS signal

In order to introduce the DBS signal to the Izhikevich model, we use the relationship [19]:

$$I_{DBS} = i_{DBS} \cdot H\left(\sin\frac{2\pi t}{\rho_{DBS}}\right) \left[1 - H\left(\sin\frac{2\pi(t + \delta_{DBS})}{\rho_{DBS}}\right)\right] \quad (5)$$

where I_{DBS} is the stimulation current, i_{DBS} corresponds to stimulation amplitude, ρ_{DBS} to stimulation period, and δ_{DBS} to the duration of each impulse. H is the Heaviside function. The general therapeutic stimulation parameters for DBS (monopolar cathodic; 1 to 5 V stimulus amplitude; 60 to 200 μ s stimulus pulse duration; 120 to 180 Hz stimulus frequency) have been derived primarily by trial and error [20].

III. RESULTS

Izhikevich models of two single neuron STN MERs (named MER-1 and MER-2, respectively), driven by LFPs, were proven to predict the spiking activity of both neurons very accurately (Fig. 1). Spiking neuron and STN neuron parameters were used for modeling MER-1 and MER-2, respectively. Value of κ , estimated to give the minimum MSE, was 8 and 4 for MER-1 and MER-2, respectively. In both cases, the model predicted the rhythm with high accuracy (for MER-1, rhythm MSE = 1.04 spikes/50 ms and for MER-2, rhythm MSE = 1.07 spikes/50 ms). For MER-1 and MER-2, the CDF plot remained inside the 92% and 95% confidence intervals, respectively. For both models, the predicted ISIs followed very accurately the recorded ones.

A constant voltage DBS signal was then superimposed to the LFPs that drive the above models. The voltage was transformed to i_{DBS} using the same κ , as before. On-DBS state of neuron was simulated using parameters that lie well inside the clinical settings of DBS.

Two simulation results, with the addition of a DBS signal (voltage amplitude 4V, pulse frequency 180 Hz and pulse duration 200 μ s) are shown in Fig. 2. For MER-1

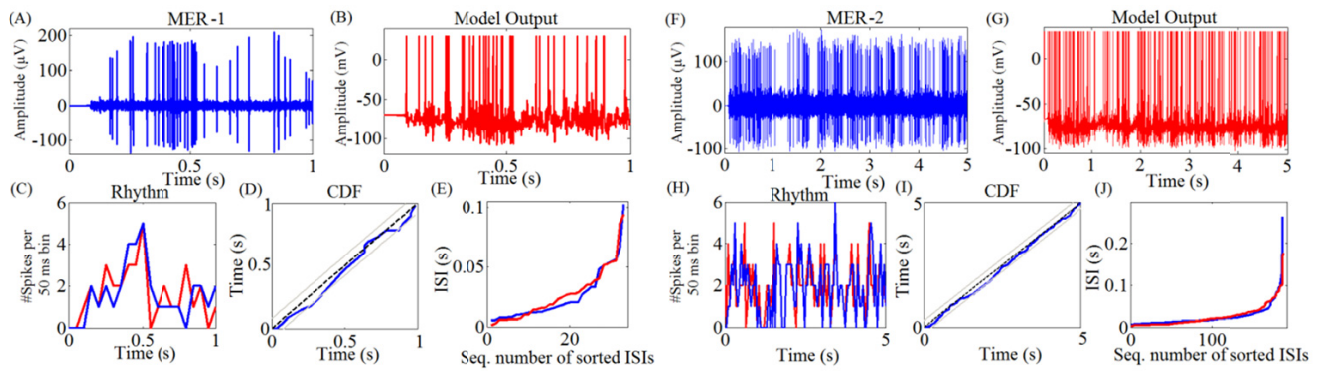


Fig. 1. Two MERs acquired from the right STN of a PD patient (male, 70 years old, UPDRS (off drugs) = 54). Final DBS location was neurologically estimated at 2 mm above the theoretical target. (A) MER-1 acquired inside the STN, 1 mm above the theoretical target. (B) Model output. (C) Spiking rhythm estimated at 50 ms bins for predicted (red) and recorded (blue) spikes. (D) The estimated CDF plot. Black dotted line represents the 45° line. Grey thick lines represent the 92% confidence interval. (E) The estimated ISIs for predicted (red) and recorded (blue) spikes. (F)-(J) as in (A)-(E) for MER-2 acquired inside the STN, 1.5 mm above the theoretical target.

(MER-2), mean firing rate increased from 1.62 (1.88) spikes/50 ms during the OFF-DBS state to 4.53 (2.27) spikes/50 ms during the ON-DBS state. In general, the STN neurons, during the ON-DBS state, fire more regularly (i.e. less pathologically) and their firing rate increases.

The effect of the DBS parameters on single neuron spiking activity was also examined. We kept two of the parameters constant and we estimated the effect of the third parameter on the spiking rhythm. To allow for the pulse width to take values in the widest possible range [90-300] µs [21], voltage amplitude was kept constant and equal to 3V. Similarly, to allow for the voltage amplitude to take values in the widest possible clinical range [2.5 – 10] V ([21], [22]), the pulse width was kept constant and equal to 80µs. For both simulations, DBS frequency was kept equal to 180 Hz. To study the effect of DBS frequency on the spiking rhythm, the pulse width was set to 150 µs and the pulse amplitude to 4 V. The results show that, in both cases, the mean firing rate increases linearly with the frequency of the pulse, its duration and its amplitude, inside the clinical range of their values. In addition, in signal segments where no neural activity was present, regular spikes were fabricated. As the parameter values increased,

the neuron's firing also became more rhythmic. This is also observed in Fig. 2 A-B, for a single set of DBS parameters.

IV. DISCUSSION

Results are in agreement with previous experimental findings demonstrating that stimulation of the glutamatergic STN output produces short-latency excitatory responses that tonically increase the average firing rate and alter the pattern of neuronal activity in both globus pallidus interna (GPI) and globus pallidus externa [23] - corresponding to the main outputs of the STN. Stimulation with parameters effective for the alleviation of rigidity and akinesia (3 V; 136 Hz) resulted in a significant increase in the mean spiking rhythm and the development of a more regular pattern of neuronal activity [23]. In addition, a research group stimulated in the GPI and recorded in thalamus of nonhuman primates. The results found are consistent with activation of the gamma-aminobutyric acidergic GPI output [24]. Their results showed a reduction in thalamic discharge frequency during GPI DBS in 77% of the responsive thalamic cells. Taken together, these data support the hypothesis that DBS increases the output of the stimulated nucleus, which directly

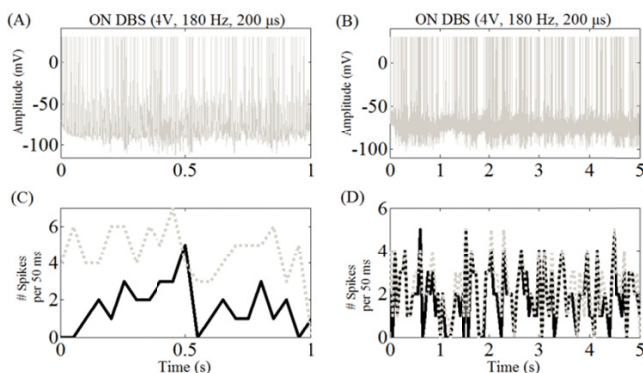


Fig. 2. Simulation of ON DBS state in two STN neurons. (A) The predicted spiking activity for MER-1 when a DBS signal is superimposed to the LFP that drives the Izhikevich model. (B) Same as in (A), for MER-2. (C) The estimated rhythm for MER-1. Black continuous (Grey dotted) curve is the OFF-DBS (ON-DBS) simulated rhythm. (D) Same as in (C), for MER-2.

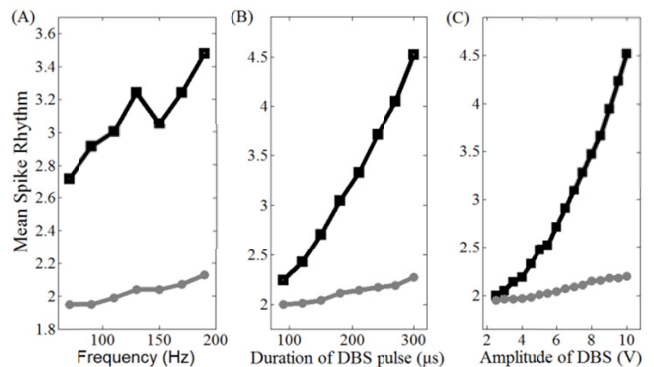


Fig. 3. Estimation of mean spike rhythm as a function of (A) pulse frequency, (B) pulse duration, and (C) pulse amplitude. Marginal clinical parameter values are included in the simulation. Note that the therapeutic range of the parameters used is less broad. Black line corresponds to the MER-1 model and grey line corresponds to the MER-2 model.

affects neural activity in output nuclei, as shown in the simulation results.

Our simulation results allow us to adopt the hypothesis that DBS modulates the activity of the basal ganglia network to “mask” the pathological firing patterns believed to characterize the Parkinsonian state ([8], [13], [19], [23]). Specifically, Parkinsonian neurons are more synchronized, rhythmic, and burstlike, when compared to normal neurons [25]. Rubin and Terman also demonstrated that a DBS signal, analogous to the one used in the present study, can elicit similarly periodic, high-frequency firing of STN and GPi cells, thereby replacing Parkinsonian firing with a mask of tonic activity [19]. The authors also show that this tonic GPi activity restores the simulated function of downstream (thalamocortical) cells that leads to the alleviation of the motor symptoms of PD.

V. CONCLUSION

In this paper, we showed that an Izhikevich model, driven by intranuclear LFPs of a PD patient, simulates accurately the timing and rhythm of single neuron STN spikes. A DBS pulse signal with clinically adjusted parameters was also include in the model in order to prove that the spiking rhythm of an STN neuron increases during ON-DBS state. We also demonstrated that DBS eliminates the bursting pattern observable in STN neurons of PD patients, by introducing regularly fabricated spikes. Our simulation results are in agreement with the current hypothesis that DBS masks the pathological firing by altering the firing pattern of the STN neurons.

ACKNOWLEDGMENT

The authors would like to thank Professor Damianos Sakas, MD for providing the data sets.

REFERENCES

- [1] J. Obeso, C. Olanow, M. Rodriguez-Oroz, P. Krack, R. Kumar, A. Lang, “Deep-brain stimulation of the subthalamic nucleus or the pars interna of the globus pallidus in Parkinson’s disease,” *N Engl J Med.*, vol. 345, pp. 956–963, 2001.
- [2] A. Benabid, P. Pollak, A. Louveau, S. Henry, J. de Rougemont, “Combined (thalamotomy, stimulation) stereotactic surgery of the VIM thalamic nucleus for bilateral Parkinson disease,” *Appl Neurophysiol.*, vol. 50, pp. 344–346, 1987.
- [3] R. Gross, A. Lozano, “Advances in neurostimulation for movement disorders,” *Neurol Res.*, vol. 22, pp. 247–258, 2000.
- [4] A. Benabid, P. Pollak, D. Gao, D. Hoffmann, P. Limousin, E. Gay, I. Payen, A. Benazzouz, “Chronic electrical stimulation of the ventralis intermedius nucleus of the thalamus as a treatment of movement disorders,” *J Neurosurg.*, vol. 84, pp. 203–214, 1996.
- [5] P. Coubes, A. Roubertie, N. Vayssiere, S. Hemm, B. Echenne, “Treatment of DYT1-generalised dystonia by stimulation of the internal globus pallidus,” *Lancet*, vol. 355, pp. 2220–2221, 2000.
- [6] M. Hodaie, R. Wennberg, J. Dostrovsky, A. Lozano, “Chronic anterior thalamus stimulation for intractable epilepsy,” *Epilepsia*, vol. 43, pp. 603–608, 2002.
- [7] L. Gabriels, P. Cosyns, B. Meyerson, S. Andreevitch, S. Sunaert, A. Maes, P. Dupont, J. Gybels, F. Gielen, H. Demeulemeester, “Long-term electrical capsular stimulation in patients with obsessive compulsive disorder,” *Neurosurgery*, vol. 52, pp. 1263–1274, 2003.

- [8] C. McIntyre, M. Savasta, B. Walter, J. Vitek, “How Does Deep Brain Stimulation Work? Present Understanding and Future Questions,” *Journal of Clinical Neurophysiology*, vol. 21, pp. 40–50, 2004.
- [9] C. Beurrier, B. Bioulac, J. Audin, C. Hammond, “High-frequency stimulation produces a transient blockade of voltage-gated currents in subthalamic neurons,” *J Neurophysiol.*, vol. 85, pp. 1351–1356, 2001.
- [10] J. Dostrovsky, R. Levy, J. Wu, W. Hutchison, R. Tasker, A. Lozano, “Microstimulation-induced inhibition of neuronal firing in human globus pallidus,” *J Neurophysiol.*, vol. 84, pp. 570–574, 2000.
- [11] F. Urbano, E. Leznik, R. Llinas, “Cortical activation patterns evoked by afferent axons stimuli at different frequencies: an in vitro voltagesensitive dye imaging study,” *Thalamus Rel Syst.*, vol. 1, pp. 371–378, 2002.
- [12] E. Montgomery, K. Baker, “Mechanisms of deep brain stimulation and future technical developments,” *Neurol Res.*, vol. 22, pp. 259–66, 2000.
- [13] A. Benabid, A. Benazzouz, P. Pollak, “Mechanisms of deep brain stimulation,” *Mov Disord.*, vol. 17(suppl 3), pp. S73–S74, 2002.
- [14] K.P. Michmizos, K.S. Nikita, “Can We Infer Subthalamic Nucleus Spike Trains from Intranuclear Local Field Potentials?,” *EMBC '10*, Buenos Aires, Argentina, September 2010.
- [15] K.P. Michmizos, D.E. Sakas, K.S. Nikita (accepted for publication) Prediction of the timing and the rhythm of the parkinsonian subthalamic nucleus neural spikes using the local field potentials *IEEE Transactions of Information Technology in Biomedicine* (TITB-00071-2011).
- [16] M. Bevan, P. Magill, D. Termanc, J. Bolamb, C. Wilson, “Move to the rhythm: oscillations in the subthalamic nucleus–external globus pallidus network,” *Trends Neurosci.*, vol. 25, pp. 525–531, 2002.
- [17] E. M. Izhikevich, “Simple model of spiking neurons,” *IEEE Trans. Neural Networks*, vol. 14, pp. 1569–1572, Nov. 2003.
- [18] P.A. Tass, “A model of desynchronizing deep brain stimulation with a demand-controlled coordinated reset of neural subpopulations,” *Biol. Cybern.*, vol. 89, pp. 81–88, 2003.
- [19] J. Rubin, D. Terman, “High frequency stimulation of the subthalamic nucleus eliminates pathological thalamic rhythmicity in a computer model,” *Journal of Computational Neuroscience*, vol. 16, pp. 211–235, 2004.
- [20] E. Moro, R. Esselink, J. Xie, M. Hommel, A. Benabid, P. Pollak, “The impact on Parkinson’s disease of electrical parameter settings in STN stimulation,” *Neurology*, vol. 59, pp. 706–713, 2002.
- [21] P. Limousin, P. Krack, P. Pollak, A. Benazzouz, C. Ardouin, D. Hoffmann, A. Benabid, “Electrical stimulation of the subthalamic nucleus in advanced Parkinson’s disease,” *N Engl J Med*, vol. 339, pp. 1105–1111, 1998.
- [22] Deep-brain stimulation for Parkinson’s Disease Study Group, “Deep-brain stimulation of the subthalamic nucleus or the pars interna of the globus pallidus in Parkinson’s disease,” *N Engl J Med*, vol. 345, pp. 956–963, 2001.
- [23] T. Hashimoto, C. Elder, M. Okun, S. Patrick, J. Vitek, “Stimulation of the subthalamic nucleus changes the firing pattern of pallidal neurons,” *J Neurosci.*, vol. 23, pp. 1916–1923, 2003.
- [24] M. Anderson, N. Postupna, M. Ruffo, “Effects of high-frequency stimulation in the internal globus pallidus on the activity of thalamic neurons in the awake monkey,” *J Neurophysiol.*, vol. 89, pp. 1150–1160, 2003.
- [25] D. Terman, J. Rubin, A. Yew, C. Wilson, “Activity patterns in a model for the subthalamopallidal network of the basal ganglia,” *J. Neurosci.*, vol. 22, pp. 2963–2976, 2002.